D-A-A' type asymmetric small molecules based on triphenylamine-diketopyrrolopyrrole/5,6-difluoro-2,1,3-benzothiadiazole backbone for organic photovoltaic materials

Lunxiang Yin, Qingqing Yuan and Yanqin Li*

*School of Chemical Engineering, Dalian University of Technology, Dalian, P. R. China.

E-mail: liyanqin@dlut.edu.cn;

Fax: +86-411-84986040; Tel: +86-411-84986040.

Supporting Information

Table of contents

1. Synthesis and characterization

1.1 Instruments

^{1}H and ^{13}C NMR spectra were performed on Bruker AVANCE II 400 MHz and 100 MHz spectrometer respectively with $CDCl_3$ as solvent, and tetramethylsilane (TMS) as the internal standard.

1.2 Synthetic procedures

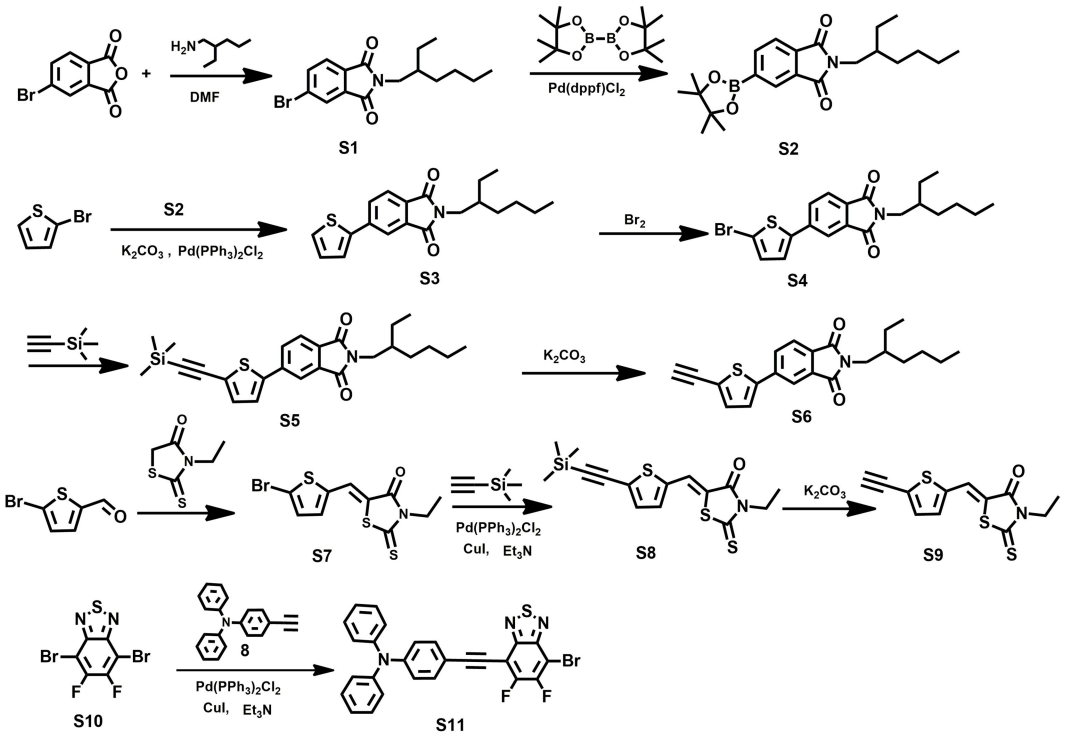

Scheme S1 The synthetic routes of intermediate compounds

Synthesis of compound S1

4-Bromophthalic anhydride (2.30 g, 10 mmol) and 2-ethylhexan-1-amine (1.6 mL, 10 mmol) were dissolved in 50 mL DMF, and the mixture was heated at 140 ^{o}C for 24 h. After being cooled to room temperature, the reaction solution was poured into 20 mL of water and extracted with ethyl acetate (3 × 20 mL). The combined organic phase was dried over anhydrous sodium sulfate. The solvent was evaporated and the residue was purified by silica column chromatography eluting with petroleum ether/ethyl acetate (10: 1) to provide a purple solid (2.30 g, 71%). Mp: 80-82 ^{o}C. ^{1}H-NMR (400 MHz, $CDCl_3$, ppm): δ d 7.97 (d, J =1.6 Hz, 1H), 7.85 (dd, J = 7.9, 1.5 Hz, 1H), 7.70 (d, J = 7.9 Hz, 1H), 3.57 (d, J = 7.3 Hz, 2H), 1.86-1.78 (m, 1H), 1.36-1.23 (m, 8H), 0.92–0.86 (m, 6H).

Synthesis of compound S2

A mixture of compound S1 (2.00 g, 6.1 mmol), bis(pinacolato)diborane (1.70 g, 6.7 mmol), $Pd(dppf)Cl_2$ (133 mg, 0.18 mmol) and potassium acetate (1.80 g, 18 mmol) in 60 mL distilled toluene was heated at 100 ^oC for 24 h. After being cooled to room temperature, the reaction solution was poured into 20 mL of water and extracted with dichloromethane (3 × 20 mL). The combined organic phase was dried over anhydrous sodium sulfate. The solvent was evaporated and the residue was purified by silica column chromatography eluting with petroleum ether/ethyl acetate (5:1) to give a pale-yellow liquid (1.66 g, 71%). ^1H-NMR (400 MHz, $CDCl_3$, ppm): δ 8.20 (s, 1H), 8.07 (d, J = 7.5 Hz, 1H), 7.74 (d, J = 7.3 Hz, 1H), 3.51 (d, J = 7.3 Hz, 2H), 1.79-1.74 (m, 1H), 1.28 (s, 12H), 1.24-1.16 (m, 8H), 0.84-0.79 (m, 6H).

Synthesis of compound S3

A mixture of compound S2 (0.50 g, 1.3 mmol), 2-Bromothiophene (0.20 g, 1.2 mmol), $Pd(PPh_3)_2Cl_2$ (86 mg, 0.12 mmol) and anhydrous potassium carbonate (3.40 g, 24 mmol) in tetrahydrofuran (20 mL) and deionized water (3.3 mL) was refluxed at 80 ^oC for 24 h. After being cooled to room temperature, the reaction solution was poured into 20 mL of water and extracted with dichloromethane (3 × 20 mL). The combined organic phase was dried over anhydrous sodium sulfate. The solvent was evaporated and the residue was purified by silica column chromatography eluting with petroleum ether/ $CHCl_2$ (1:2) to obtain 0.28 g pale-yellow liquid in a yield of 66%. ^1H NMR (400 MHz, $CDCl_3$) δ 8.06 (s, 1H), 7.91 (d, J = 7.8 Hz, 1H), 7.82 (d, J = 7.8 Hz, 1H), 7.49 (d, J = 3.3 Hz, 1H), 7.42 (d, J = 5.0 Hz, 1H), 7.15 (d, J = 4.3 Hz, 1H), 3.59 (d, J = 7.0 Hz, 2H), 1.75-1.92 (m, 1H), 1.22-1.40 (m, 8H), 0.93-0.87 (m, 6H).

Synthesis of compound S4

The compound S3 (0.28 g, 0.81 mmol) was dissolved in 40 mL chloroform. A mixture of Br_2 (0.045 ml, 0.89 mmol) and 20 mL chloroform was added dropwise to the flask at 0 ^oC. The reaction mixture was stirred at room temperature overnight in the dark. The reaction solution was quenched by saturated sodium bisulfite solution and extracted with chloroform (3 × 20 mL). The combined organic phase was dried over anhydrous sodium sulfate. The solvent was evaporated and the residue was purified by silica column chromatography eluting with petroleum ether/ $CHCl_2$ (1:1) to provide a purple solid in (0.30 g, 88%). M.p.: 96-97 ^oC. ^1H NMR (400 MHz, $CDCl_3$) δ 7.89 (s, 1H), 7.70-7.79 (m, 2H), 7.16 (d, J = 3.8 Hz, 1H), 7.03 (d, J = 3.8 Hz, 1H), 3.52

(d, *J* = 7.3 Hz, 2H), 1.72-1.83 (m, 1H), 1.10-1.35 (m, 8H), 0.79-0.88 (m, 6H).

Synthesis of compound S5

A mixture of compound S4 (0.29 g, 0.69 mmol), trimethylsilyl acetylene (0.11 mL, 0.76 mmol), $Pd(PPh_3)_2Cl_2$ (24 mg, 0.035 mmol) and CuI (13 mg, 0.069 mmol) in tetrahydrofuran (10 mL) and triethylamine (3 mL) was refluxed at 70 ^oC for 12 h. After being cooled to room temperature, the reaction solution was poured into 20 mL of water and extracted with chloroform (3 × 20 mL). The combined organic phase was dried over anhydrous sodium sulfate. The solvent was evaporated and the residue was purified by silica column chromatography eluting with petroleum ether/$CHCl_2$ (1:1) to obtain 0.26 g purple solid in a yield of 83%. M.p.: 90-91 ^oC. ^1H NMR (400 MHz, $CDCl_3$) δ 8.00 (s, 1H), 7.80-7.87 (m, 2H), 7.32 (d, *J* = 3.8 Hz, 1H), 7.23 (d, *J* = 3.8 Hz, 1H), 3.59 (d, *J* = 7.3 Hz, 2H), 1.82-1.90 (m, 1H), 1.36-1.26 (m, 8H), 0.87-0.99 (m, 6H), 0.27 (s, 9H).

Synthesis of compound S6

K_2CO_3 (0.82 g, 5.9 mmol) was added to a solution of compound S5 (0.25 g, 0.60 mmol) in tetrahydrofuran (10 ml) and methanol (3 mL), and the mixture was stirred 4 h at room temperature. Then the precipitate was filtered off and filtrate was collected. After removing the solvent under reduced pressure, the residue was purified by silica column chromatography eluting with petroleum ether/ $CHCl_2$ (1:1) to obtain 0.12 g purple solid in a yield of 53%. M.p.: 94-95 ^oC. ^1H NMR (400 MHz, $CDCl_3$) δ 8.02 (s, 1H), 7.82-7.88 (m, 2H), 7.34 (d, *J* = 3.8 Hz, 1H), 7.29 (d, *J* = 3.8 Hz, 1H), 3.59 (d, *J* = 7.3 Hz, 2H), 3.47 (s, 1H), 1.87-1.82 (m, 1H), 1.25-1.35 (m, 8H), 0.85-0.94 (m, 6H).

Synthesis of compound S7

A mixture of 5-Bromo-2-thiophenecarbaldehyde (0.20 g, 1.0mmol), 3-ethylrhodanine (0.25 g, 1.6 mmol) in chloroform (30 mL) and triethylamine (4 mL) was refluxed at 60 ^oC for 12 h. After being cooled to room temperature, the reaction solution was poured into 20 mL of water and extracted with chloroform (3 × 20 mL). The combined organic phase was dried over anhydrous sodium sulfate. The solvent was evaporated and the residue was purified by silica column chromatography eluting with petroleum ether/$CHCl_2$ (1:2) to provide a purple solid (0.31 g, 89%) . M.p.: 157-158 ^oC. ^1H NMR (400 MHz, $CDCl_3$) δ 7.68 (s, 1H), 7.08 (d, *J* = 7.0 Hz 2H), 4.11 (q, *J* = 7.2 Hz, 2H), 1.21 (t, *J* = 7.1 Hz, 3H).

Synthesis of compound S8

A mixture of compound S7 (0.20 g, 0.60 mmol), trimethylsilyl acetylene (0.10 ml, 0.66 mmol), $Pd(PPh_3)_2Cl_2$ (21 mg, 0.030 mmol) and CuI (12 mg, 0.060 mmol) in tetrahydrofuran (20 mL) and triethylamine (3 mL) was refluxed for at 70 ^oC 12 h. After being cooled to room temperature, the reaction solution was poured into 20 mL of water and extracted with chloroform (3 × 20 mL). The combined organic phase was dried over anhydrous sodium sulfate. The solvent was evaporated and the residue was purified by silica column chromatography eluting with petroleum ether/$CHCl_2$ (1:1) to obtain 0.14 g purple solid in a yield of 66%. M.p.: 173-174 ^oC.^1H NMR (400 MHz, $CDCl_3$) δ 7.72 (s, 1H), 7.17 (d, *J* = 7.0 Hz 2H), 4.11 (q, *J* = 7.2 Hz, 2H), 1.22 (t, *J* = 7.1 Hz, 3H), 0.20 (s, 9H).

Synthesis of compound S9

K_2CO_3 (1.90 g, 14.0 mmol) was added to a solution of compound S8 (0.50 g, 1.40 mmol) in tetrahydrofuran (15 mL) and methanol (6 mL), and the mixture was stirred at room temperature for 10 min. Then the precipitate was filtered off and filtrate was collected. After removing the solvent under reduced pressure, the residue was purified by silica column chromatography eluting with petroleum ether/ $CHCl_2$ (1:1) to give a purple solid (0.21 g , 53%) . M.p.: 119-120 ^oC. ^1H NMR (400 MHz, $CDCl_3$) δ 7.72 (s, 1H), 7.23 (d, *J* = 3.8 Hz, 1H), 7.17 (d, *J* = 3.8 Hz, 1H), 4.11 (q, J = 7.1 Hz, 2H), 3.54 (s, 1H), 1.22 (t, *J* = 7.0 Hz, 3H).

Synthesis of compound S10

Compound 10 was synthesized according to the reported procedures[1].

Synthesis of compound S11

Compound 10 (0.62 g, 1.9 mmol), compound 8 (0.43 g, 1.6 mmol), $Pd(PPh_3)_2Cl_2$ (28 mg, 0.039 mmol) and CuI (15 mg, 0.079 mmol) were dissolved in tetrahydrofuran (15 mL) and triethylamine (6.0 mL) , and the mixture was refluxed at 70 °C under nitrogen atmosphere for 12 h. After being cooled to room temperature, the reaction solution was poured into 20 mL of water and extracted with dichloromethane (3 × 20 mL). The combined organic phase was dried over anhydrous sodium sulfate. The solvent was evaporated and the residue was purified by silica column chromatography eluting with petroleum ether/CH_2Cl_2 (1:2) to afford a purple solid (0.28 g, 34%) . M.p.: 169-170 °C. ^1H-NMR (400 MHz, $CDCl_3$) δ 7.51 (d, *J* = 8.7 Hz, 2H), 7.32-7.28 (m, 4H), 7.09-7.16 (m, 7.5 Hz, 6H), 7.03 (d, *J* = 8.7 Hz, 2H).

2. ^{1}H NMR and ^{13}C NMR spectra

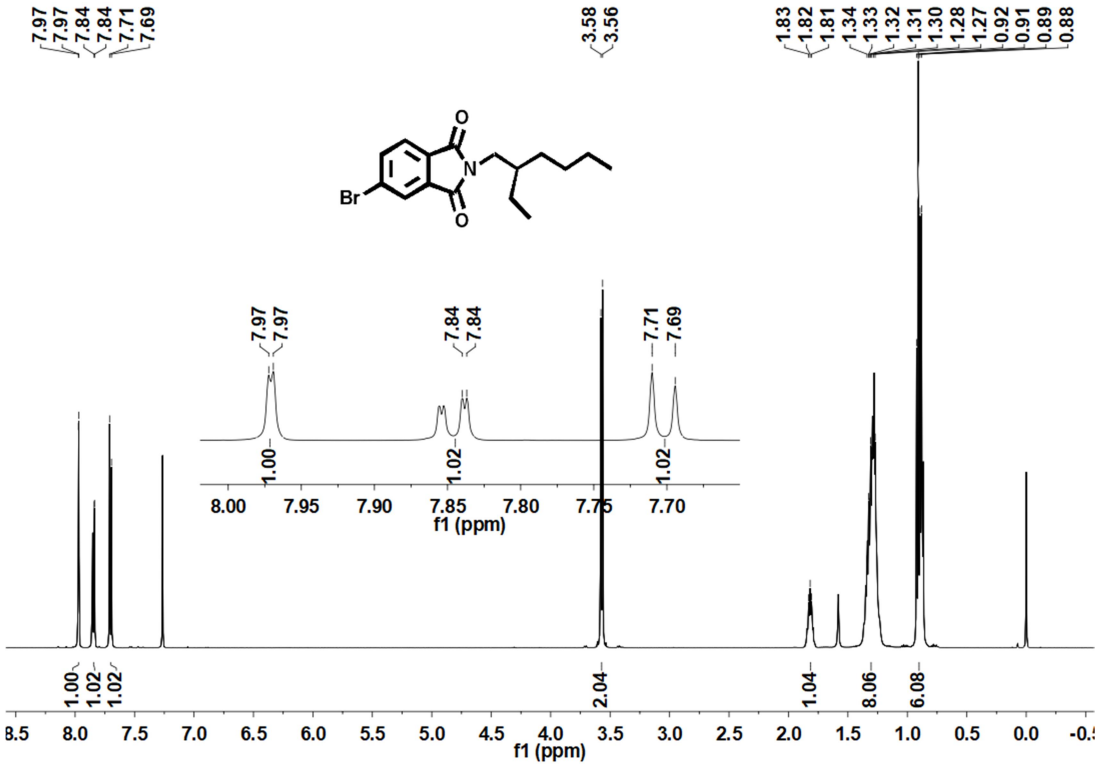

Fig. S1 ^{1}H NMR spectrum of compound **S1**

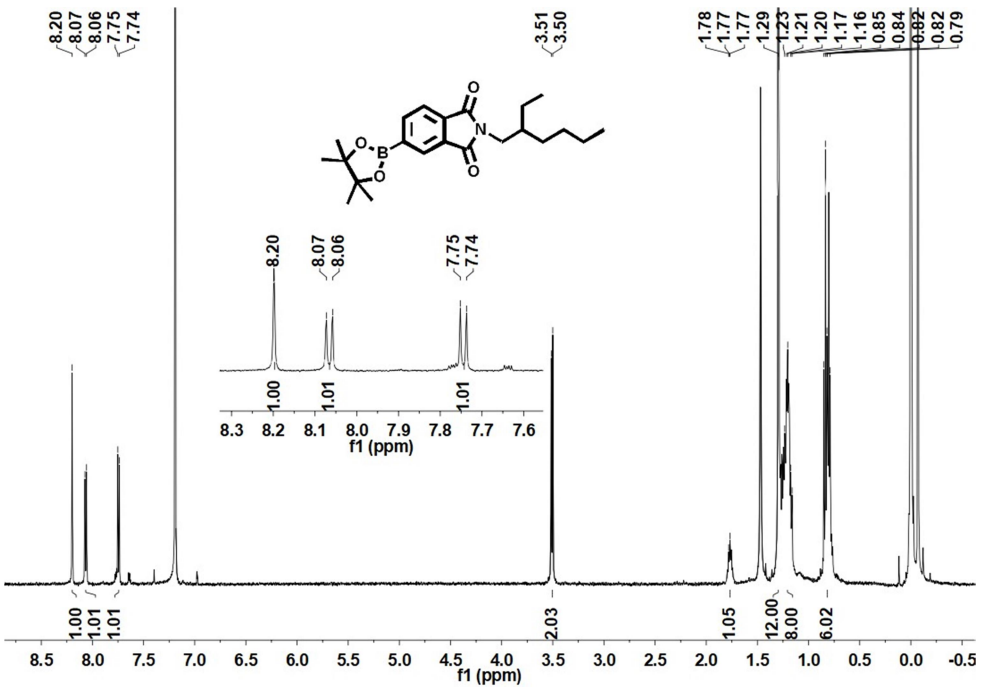

Fig. S2 ^{1}H NMR spectrum of compound **S2**

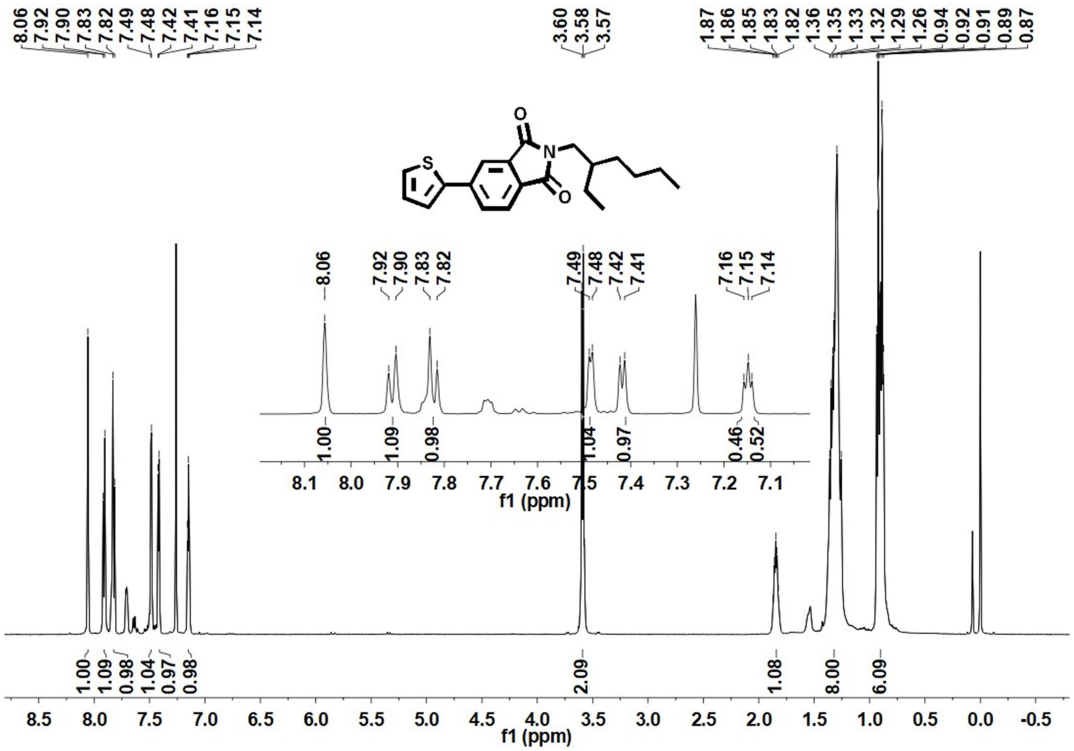

Fig. S3 ^{1}H NMR spectrum of compound **S3**

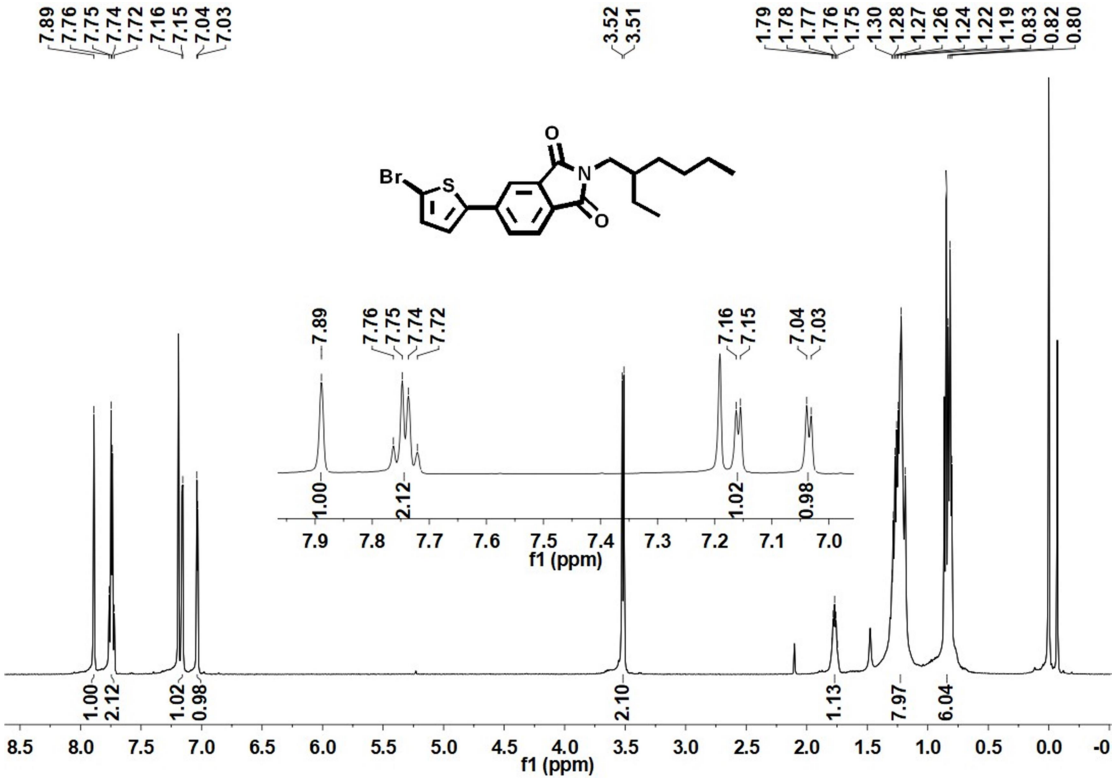

Fig. S4 ^{1}H NMR spectrum of compound **S4**

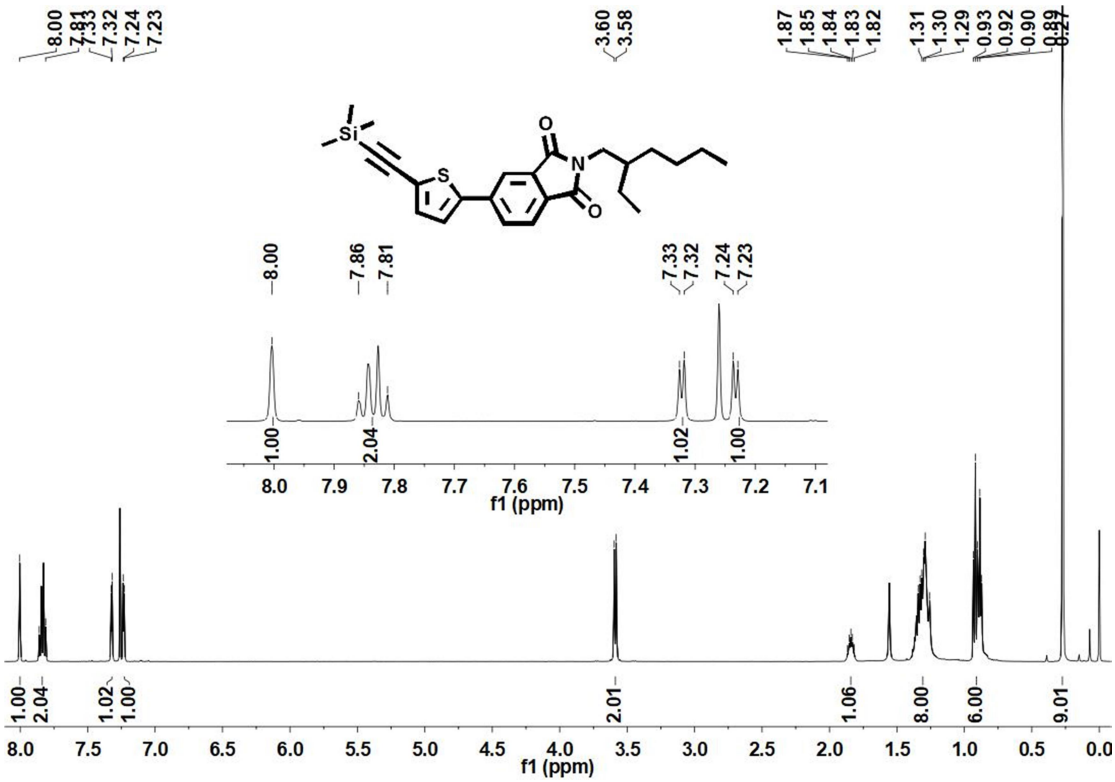

Fig. S5 ^{1}H NMR spectrum of compound **S5**

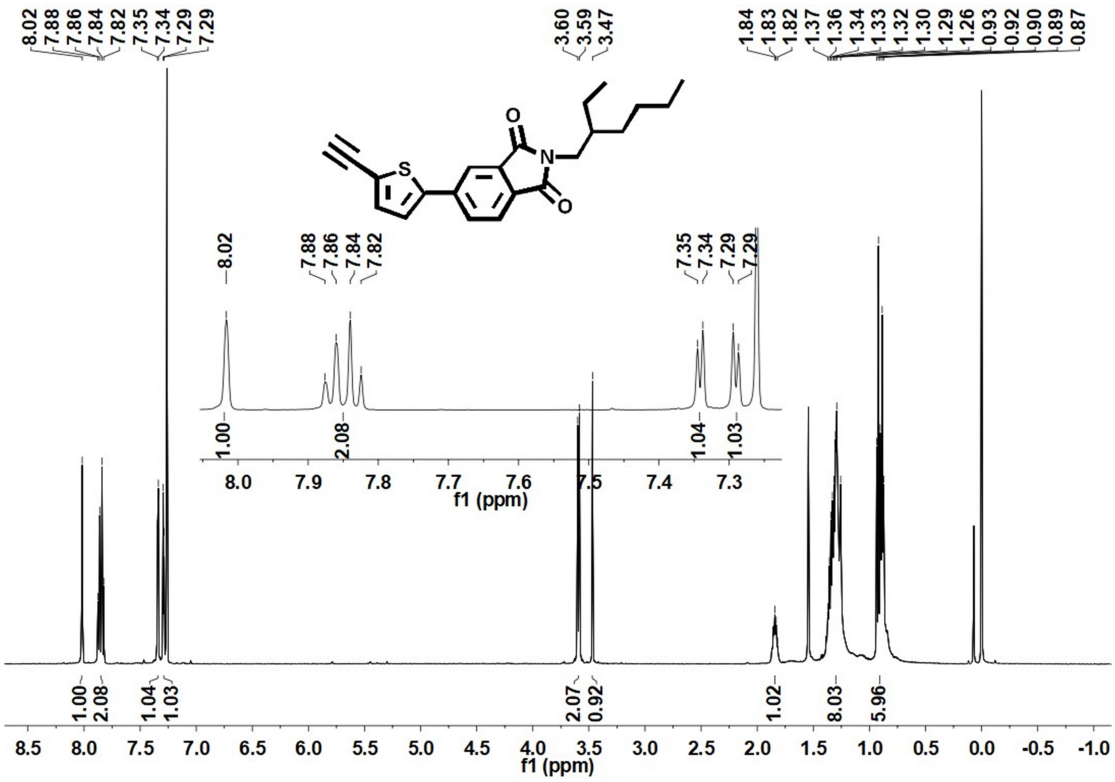

Fig. S6 ^{1}H NMR spectrum of compound **S6**

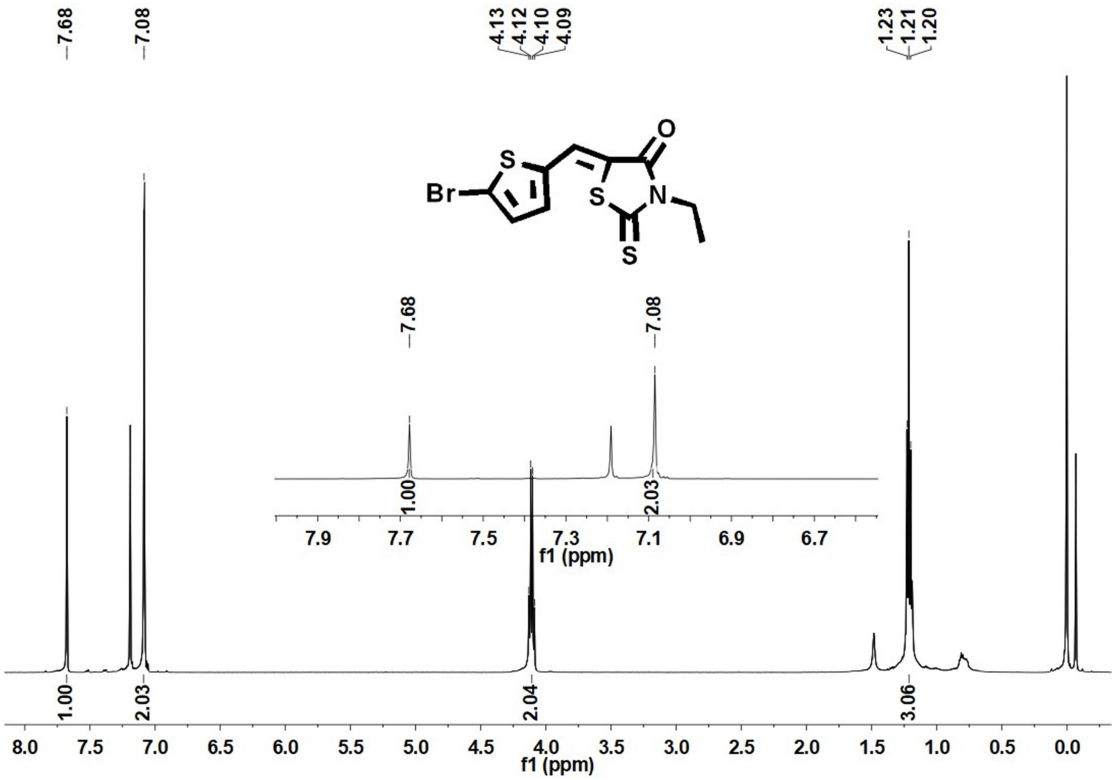

Fig. S7 ^{1}H NMR spectrum of compound **S7**

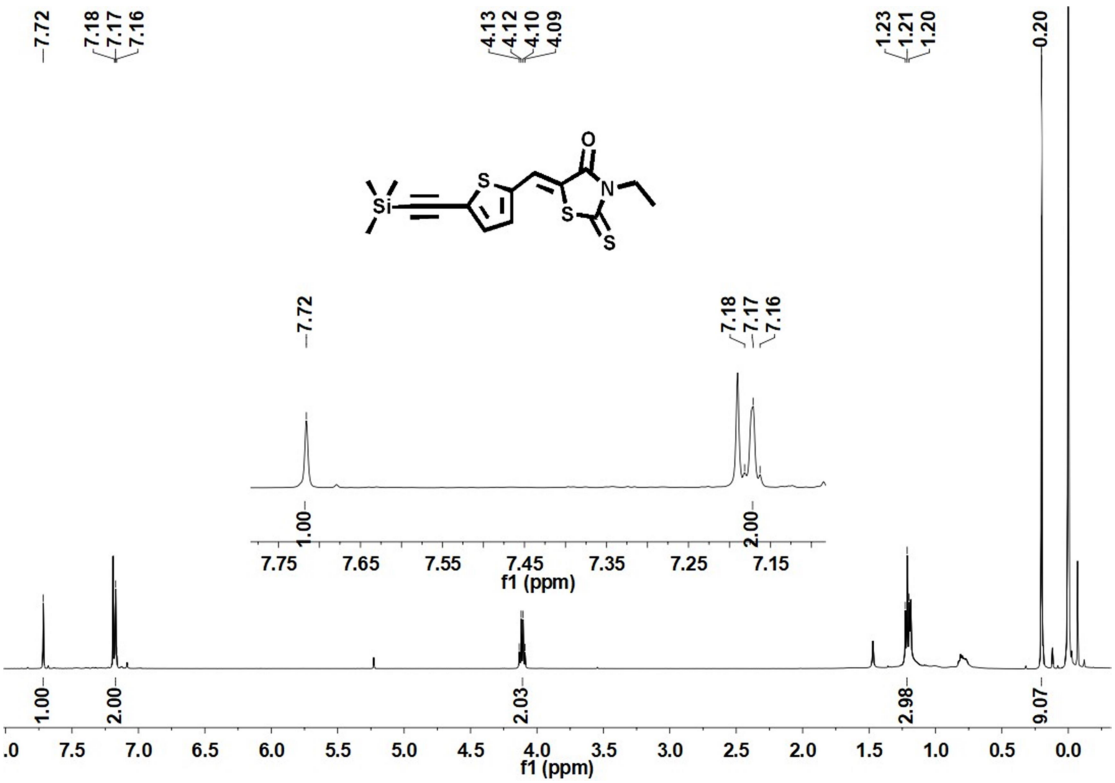

Fig. S8 ^{1}H NMR spectrum of compound **S8**

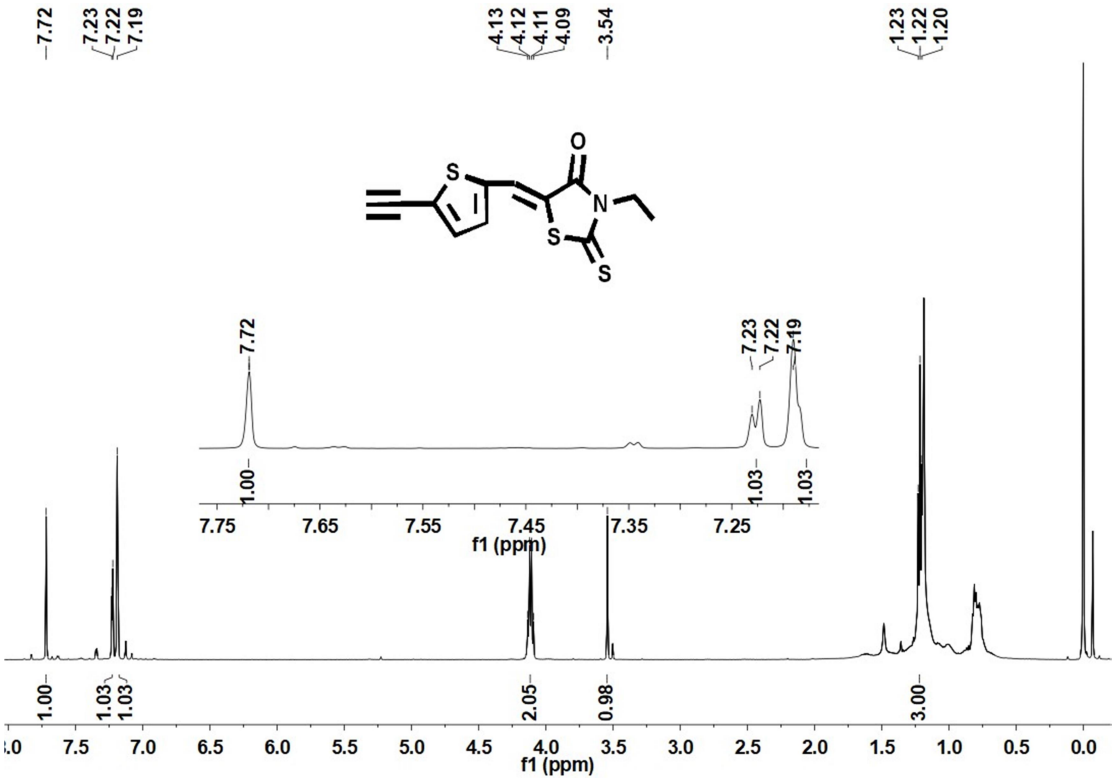

Fig. S9 ^{1}H NMR spectrum of compound **S9**

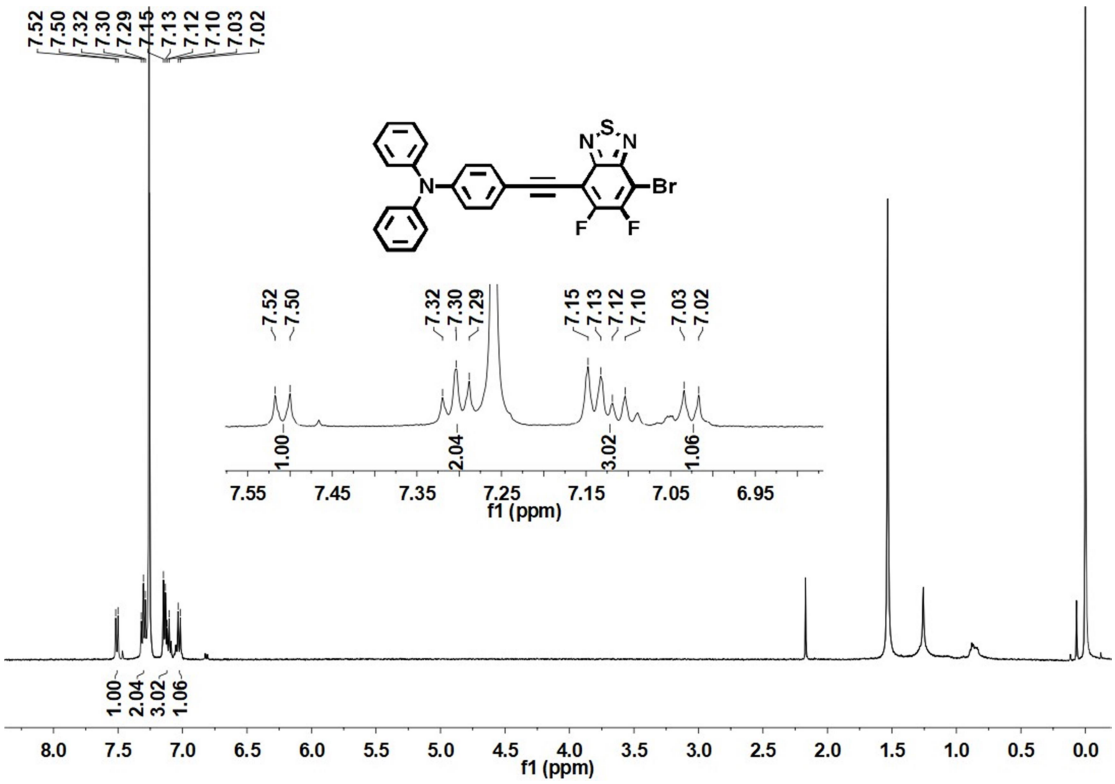

Fig. S10 ^{1}H NMR spectrum of compound **S11**

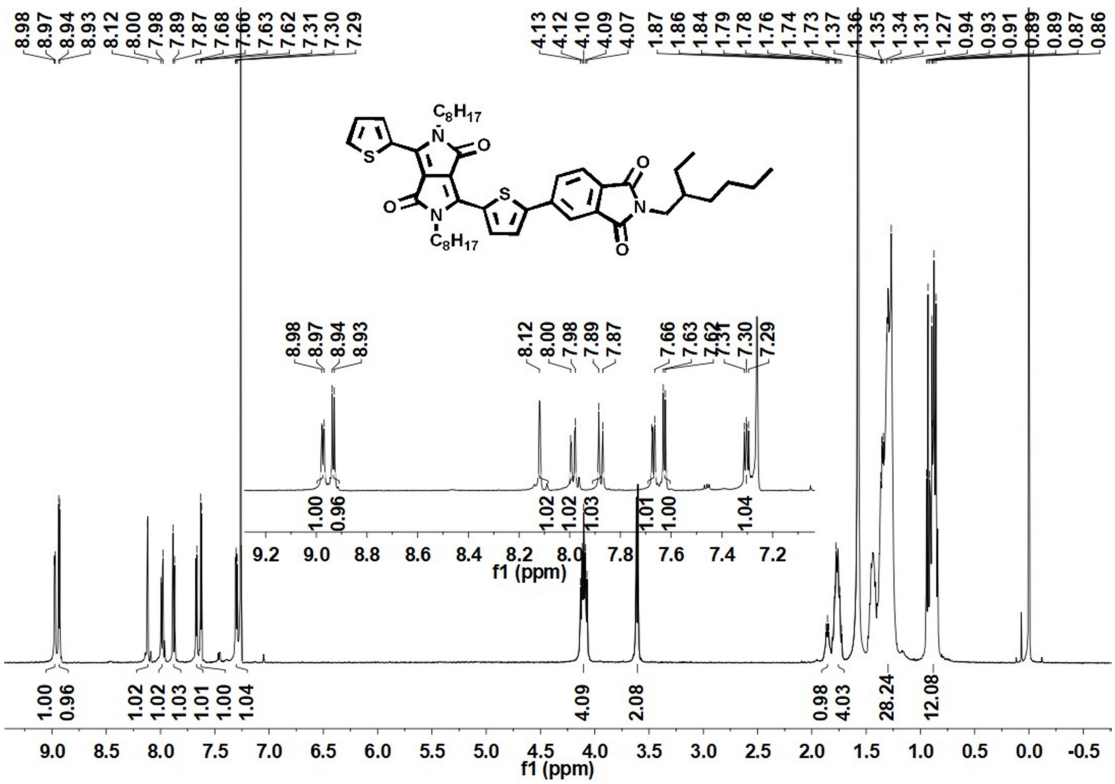

Fig. S11 ^{1}H NMR spectrum of compound **3**

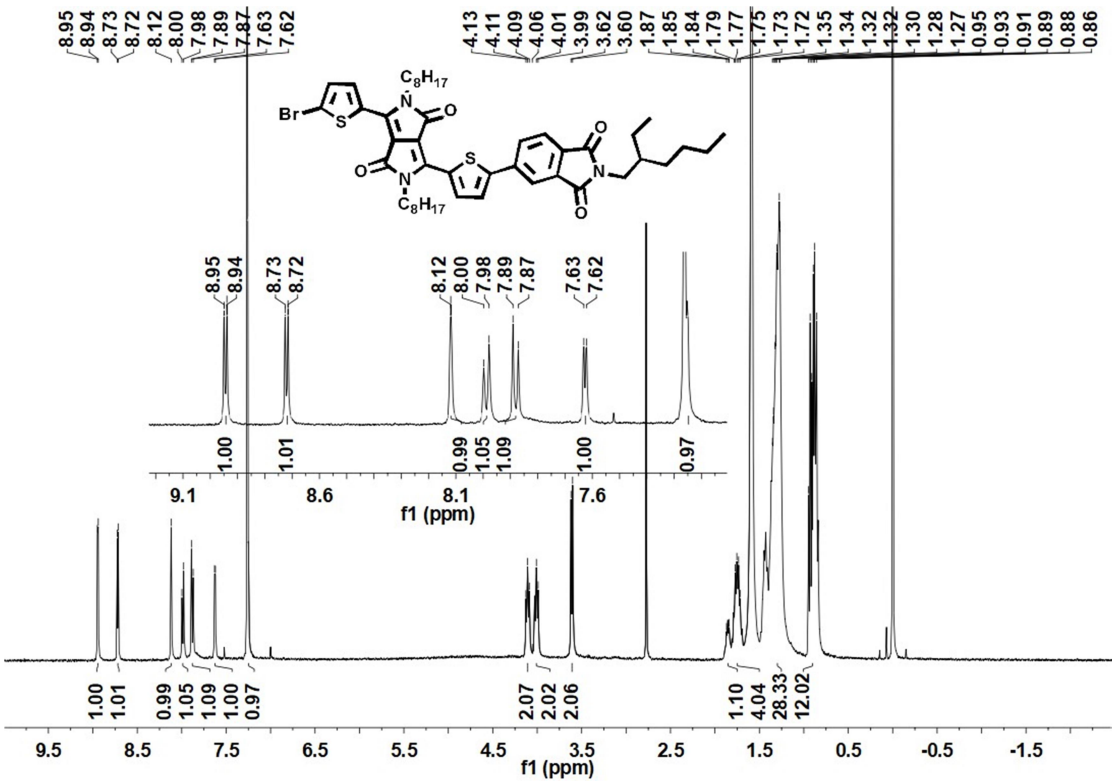

Fig. S12 ^{1}H NMR spectrum of compound **4**

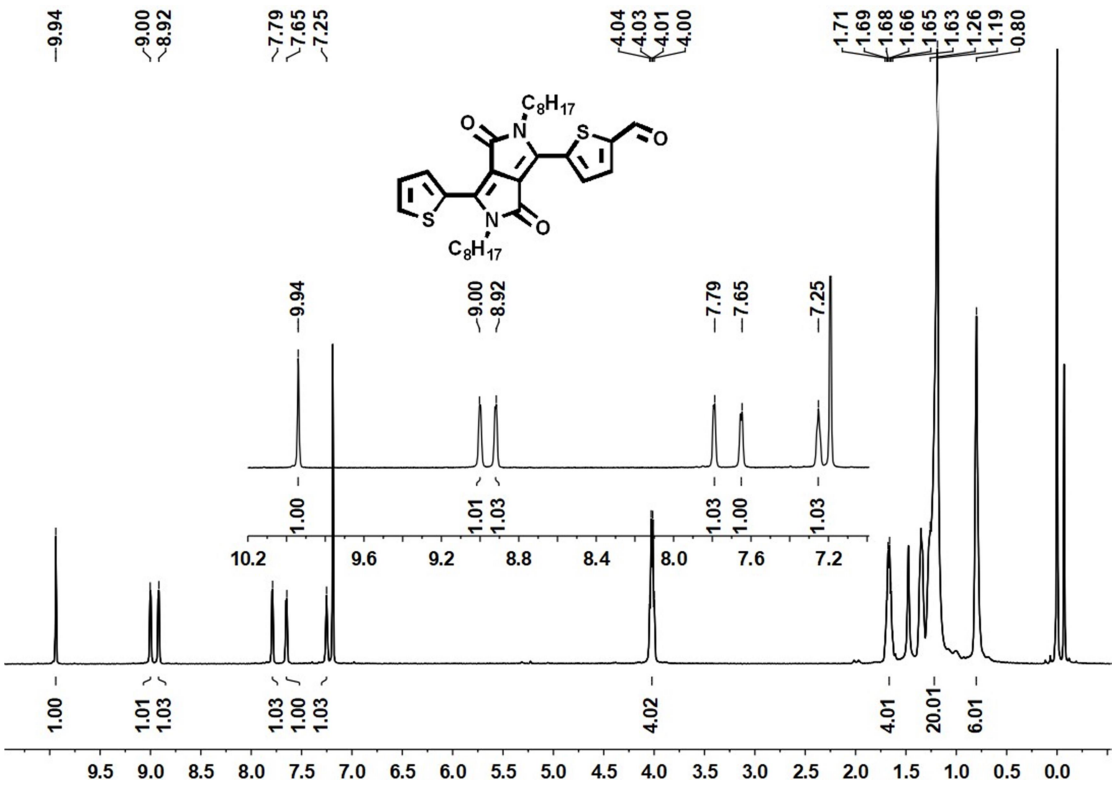

Fig. S13 ^{1}H NMR spectrum of compound **5**

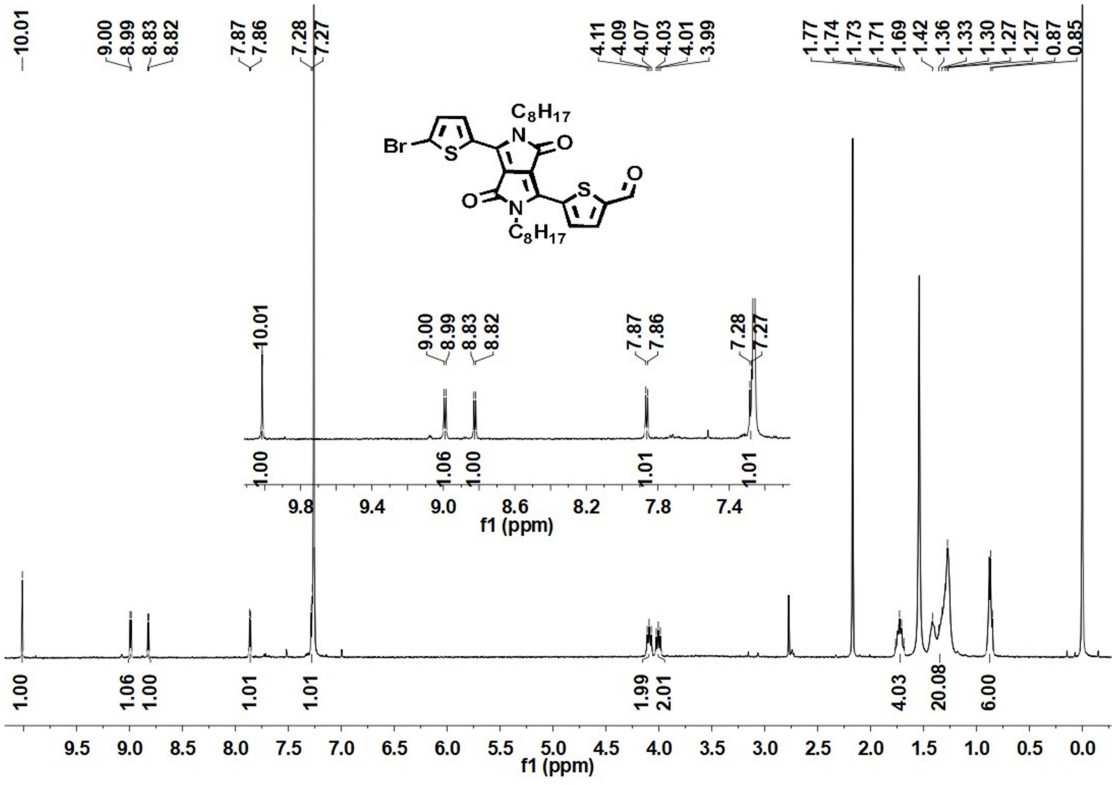

Fig. S14 ^{1}H NMR spectrum of compound **6**

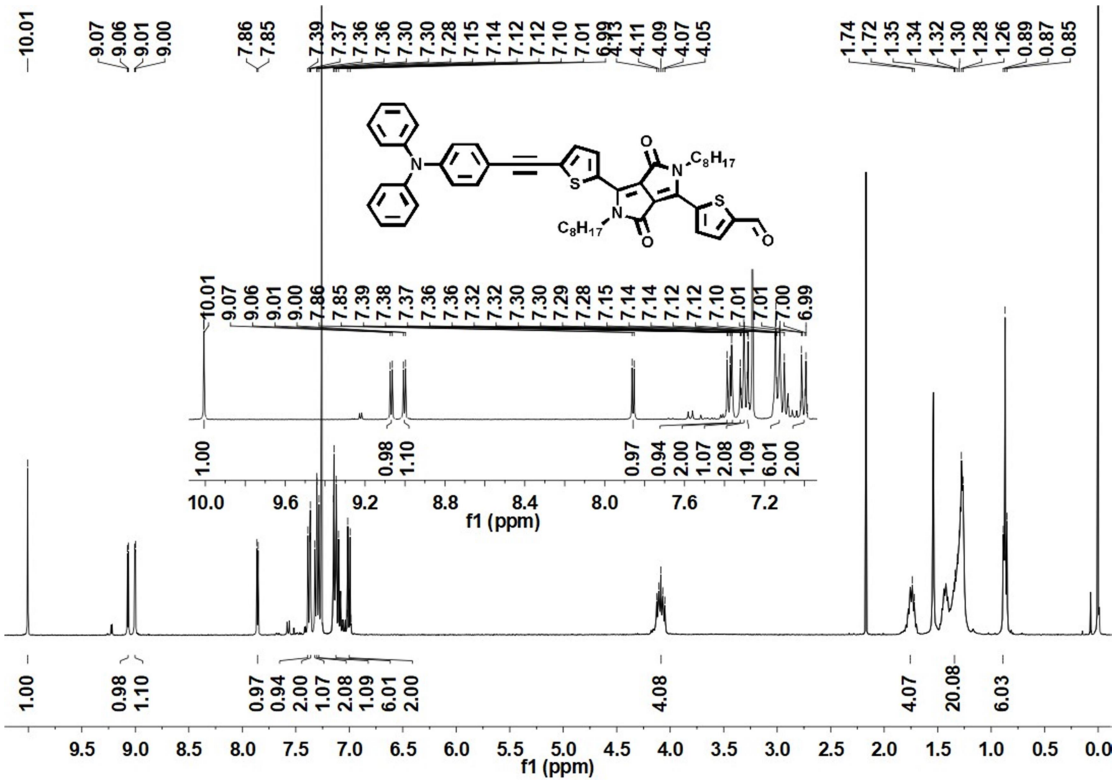

Fig. S15 ^{1}H NMR spectrum of compound **7**

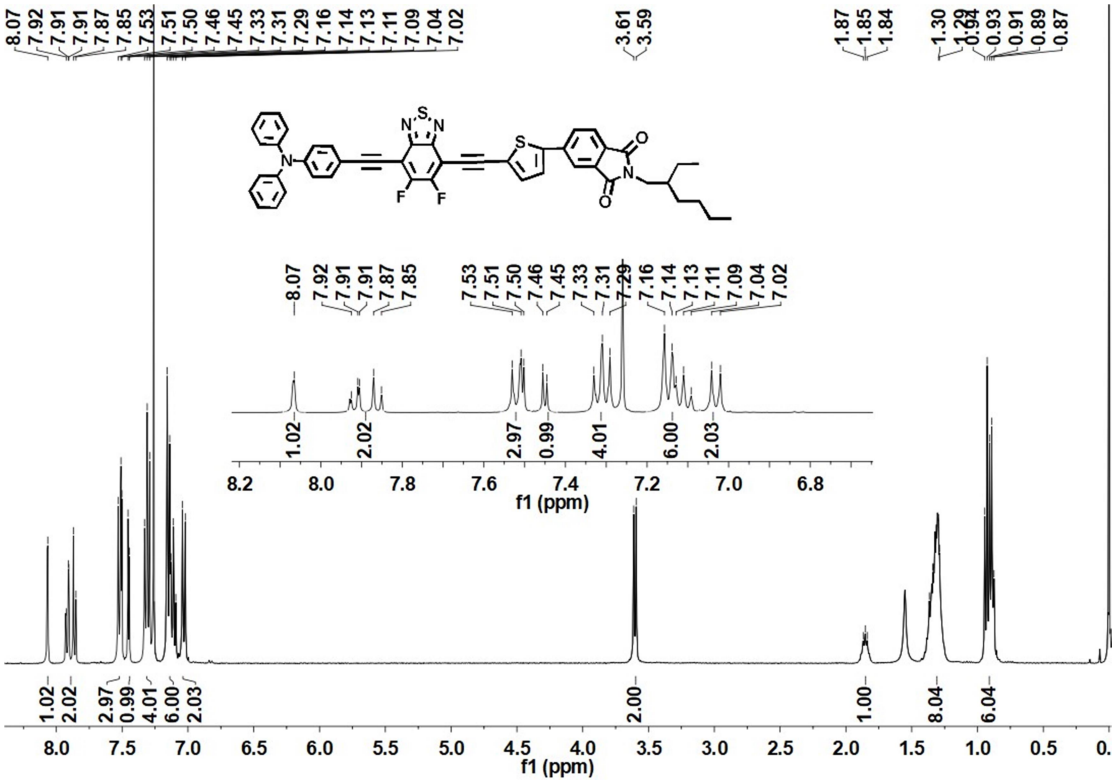

Fig. S16 ^{1}H NMR spectrum of **BT-1**

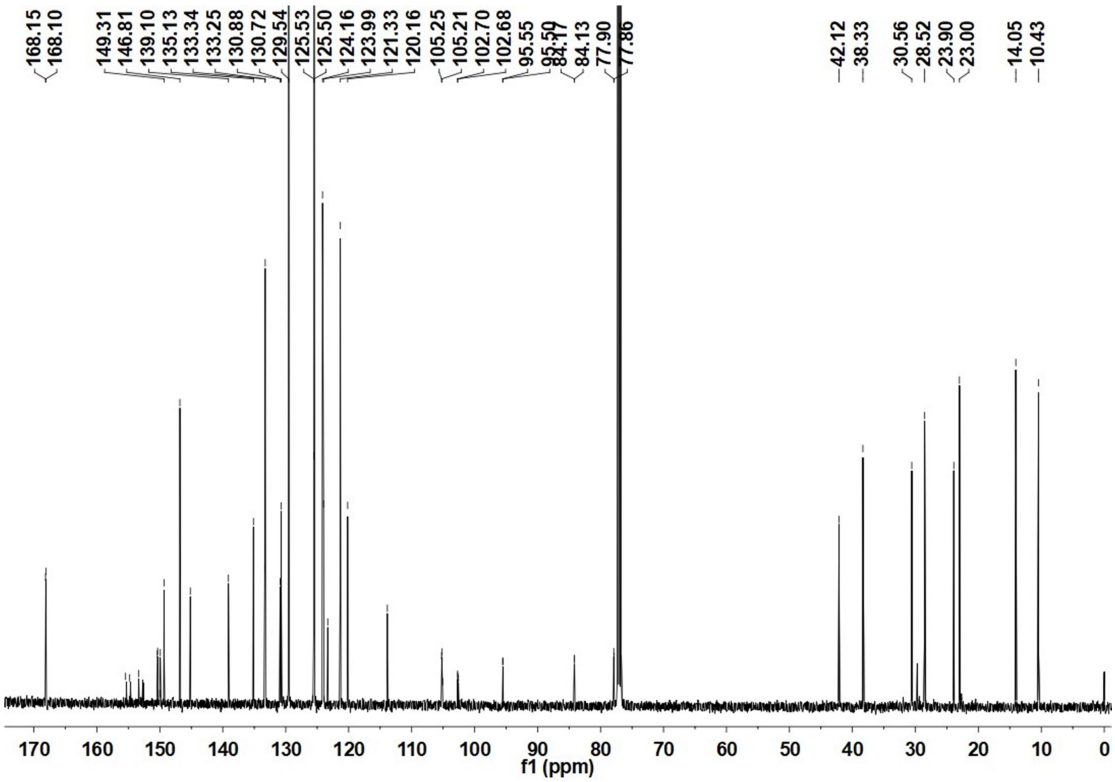

Fig. S17 ^{13}C NMR spectrum of **BT-1**

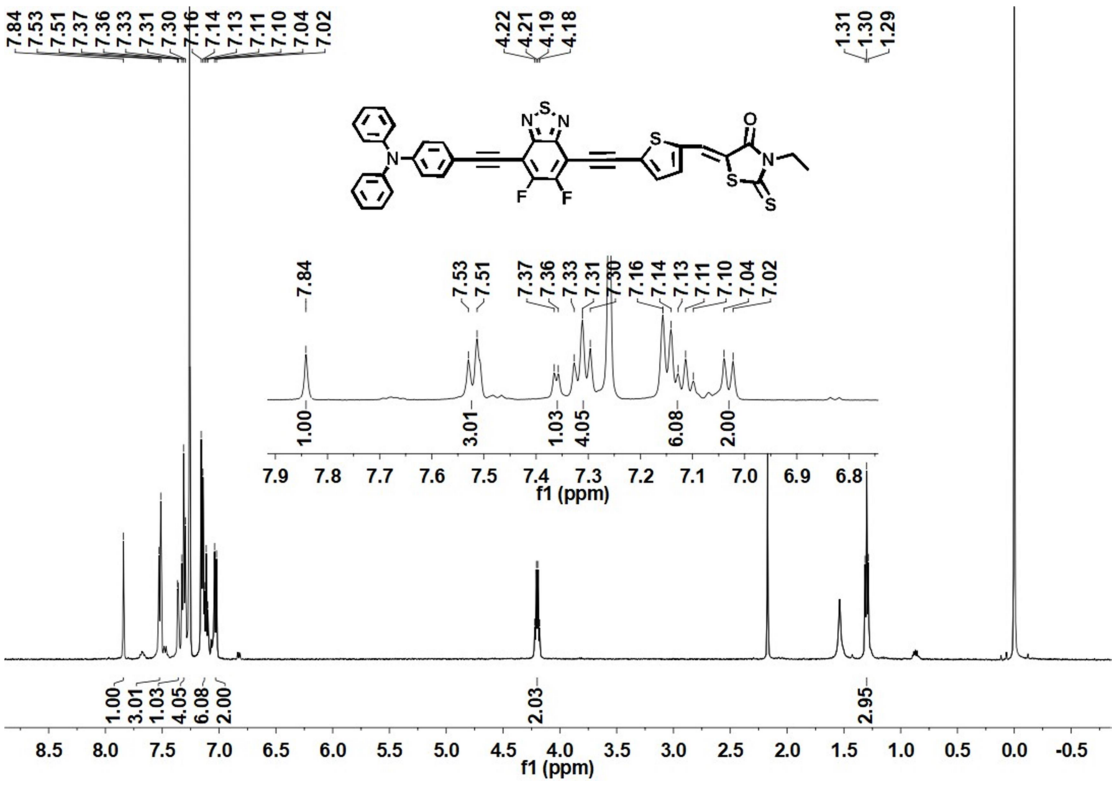

Fig. S18 ^{1}H NMR spectrum of **BT-2**

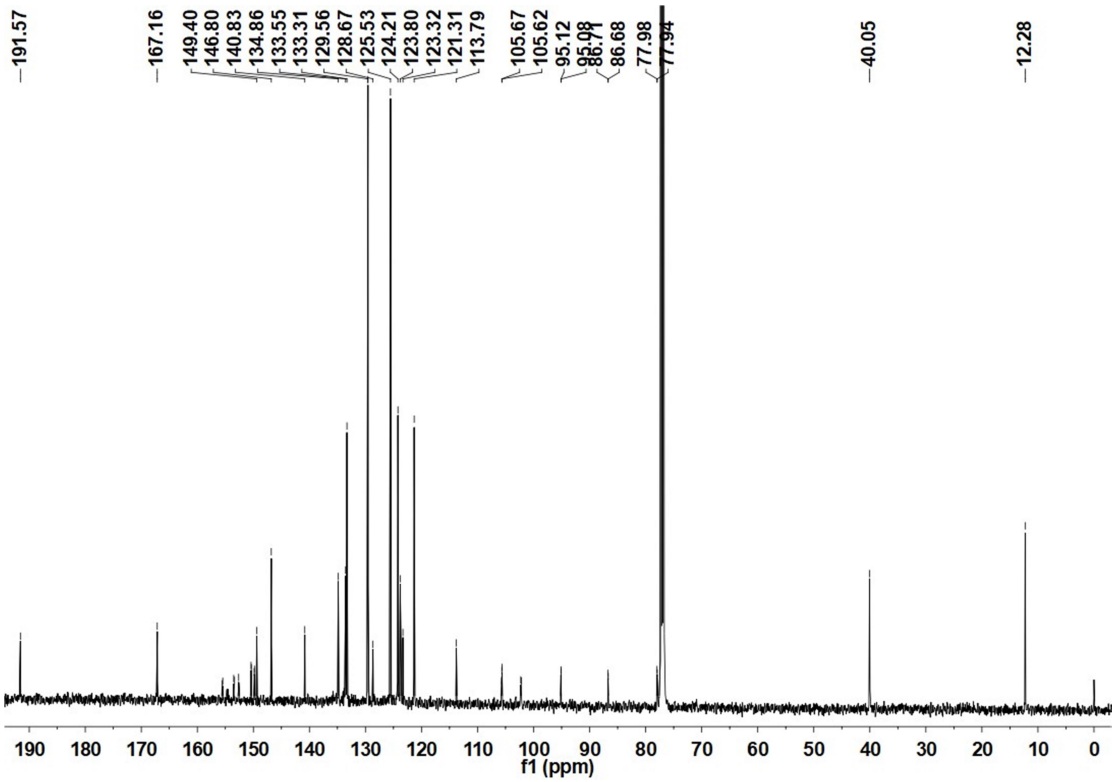

Fig. S19 ^{13}C NMR spectrum of **BT-2**

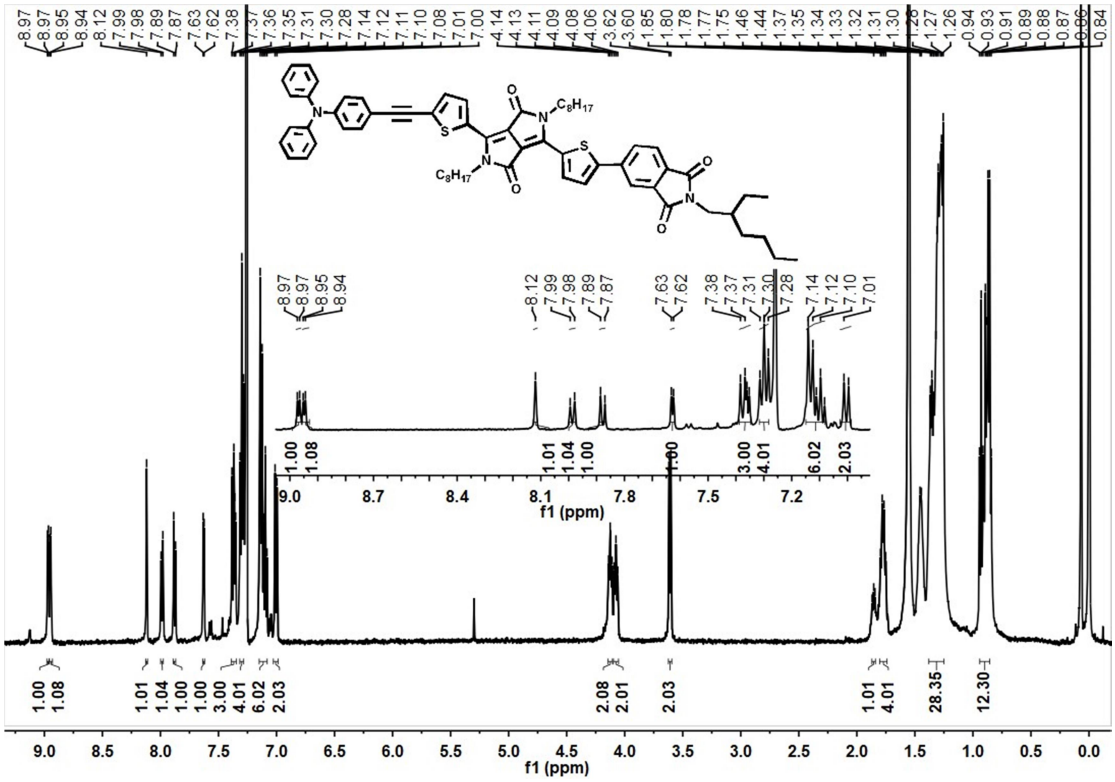

Fig. S20 ^{1}H NMR spectrum of **DPP-1**

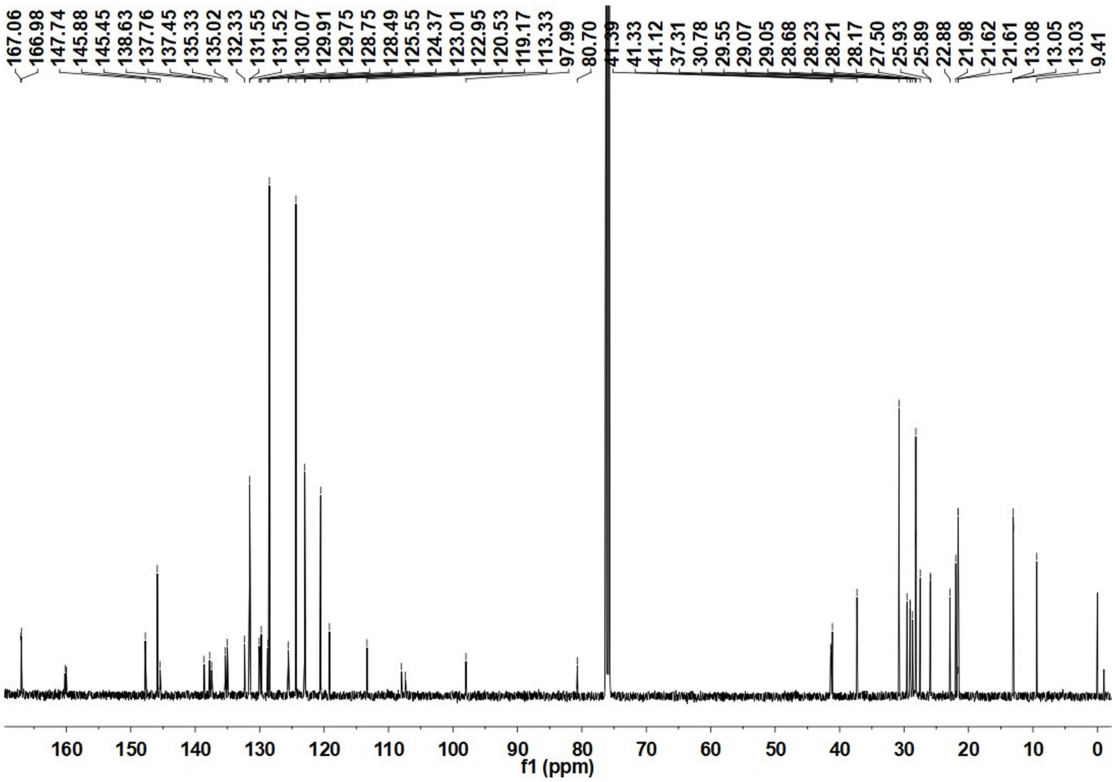

Fig. S21 ^{13}C NMR spectrum of **DPP-1**

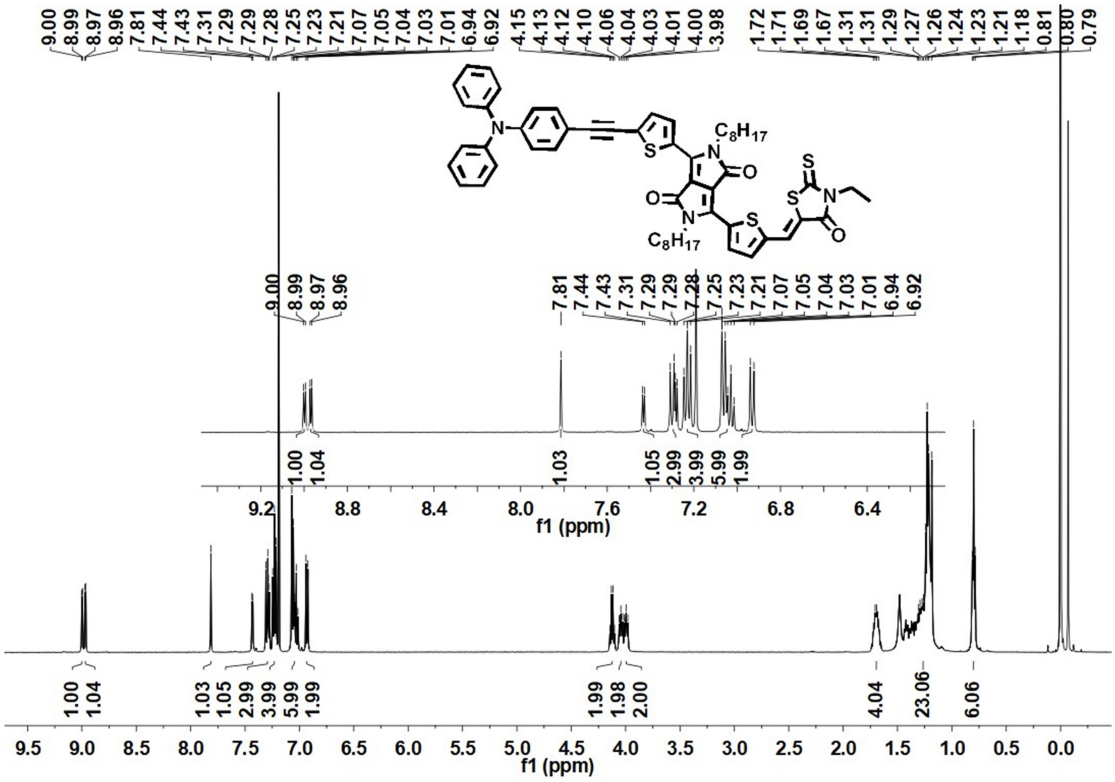

Fig. S22 ^{1}H NMR spectrum of **DPP-2**

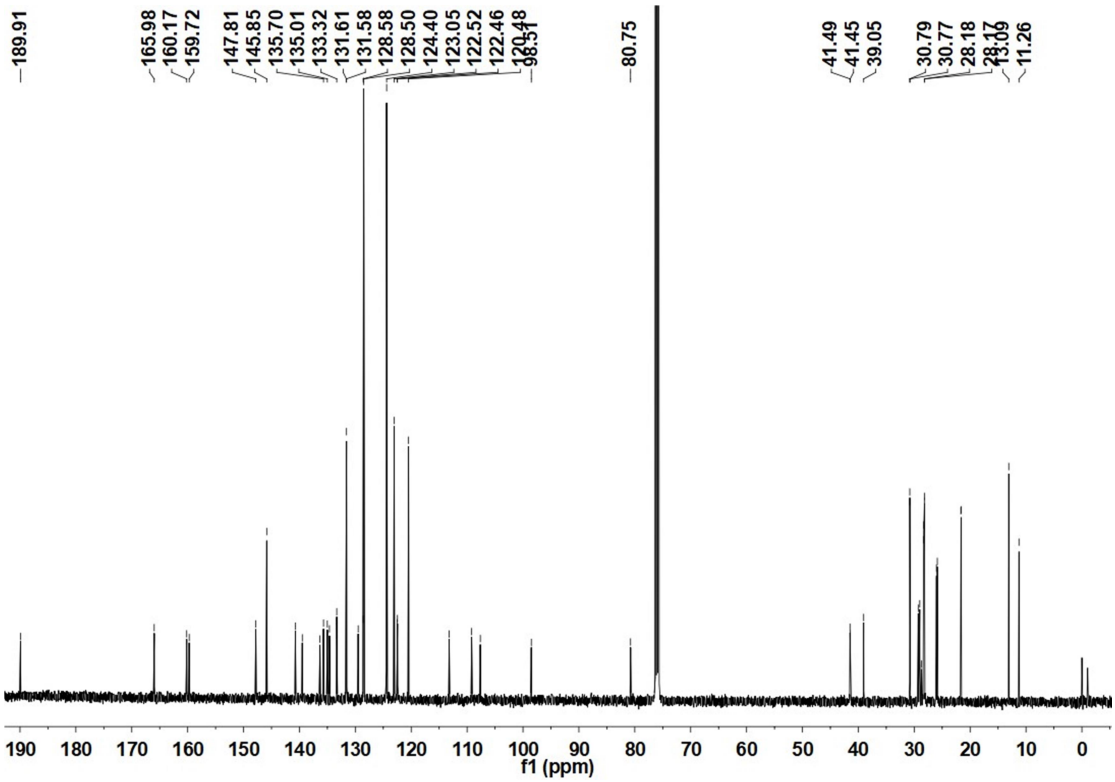

Fig. S23 ^{13}C NMR spectrum of **DPP-2**

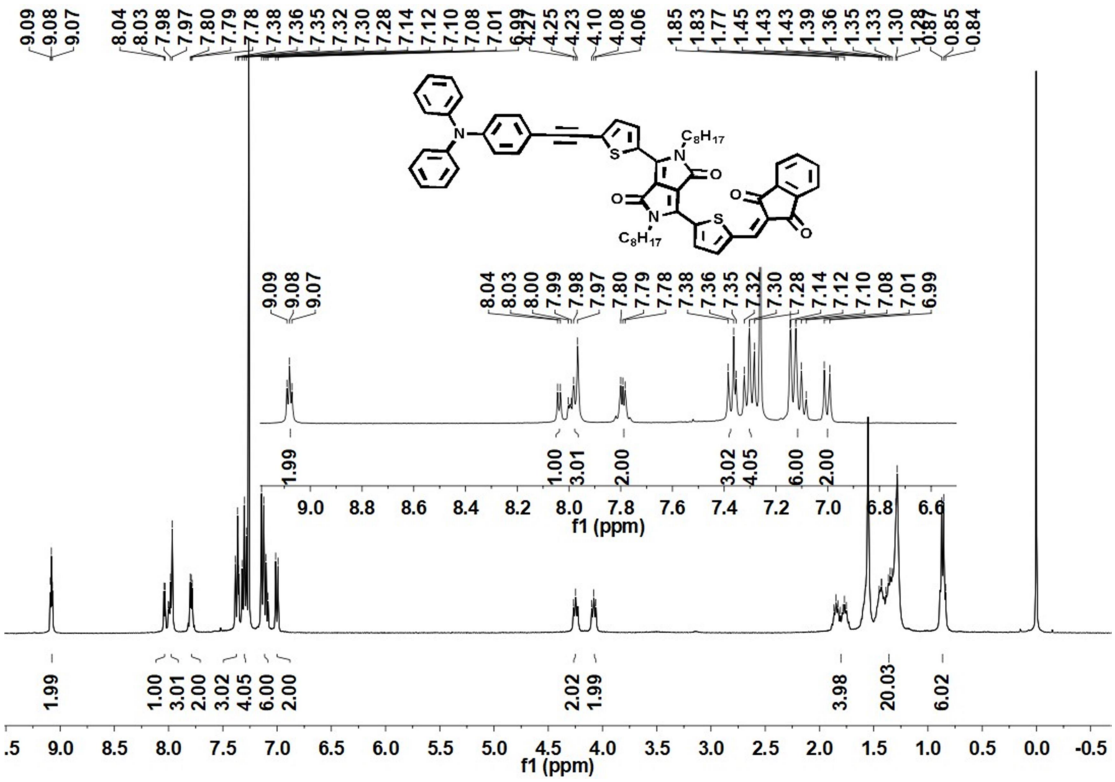

Fig. S24 ^{1}H NMR spectrum of **DPP-3**

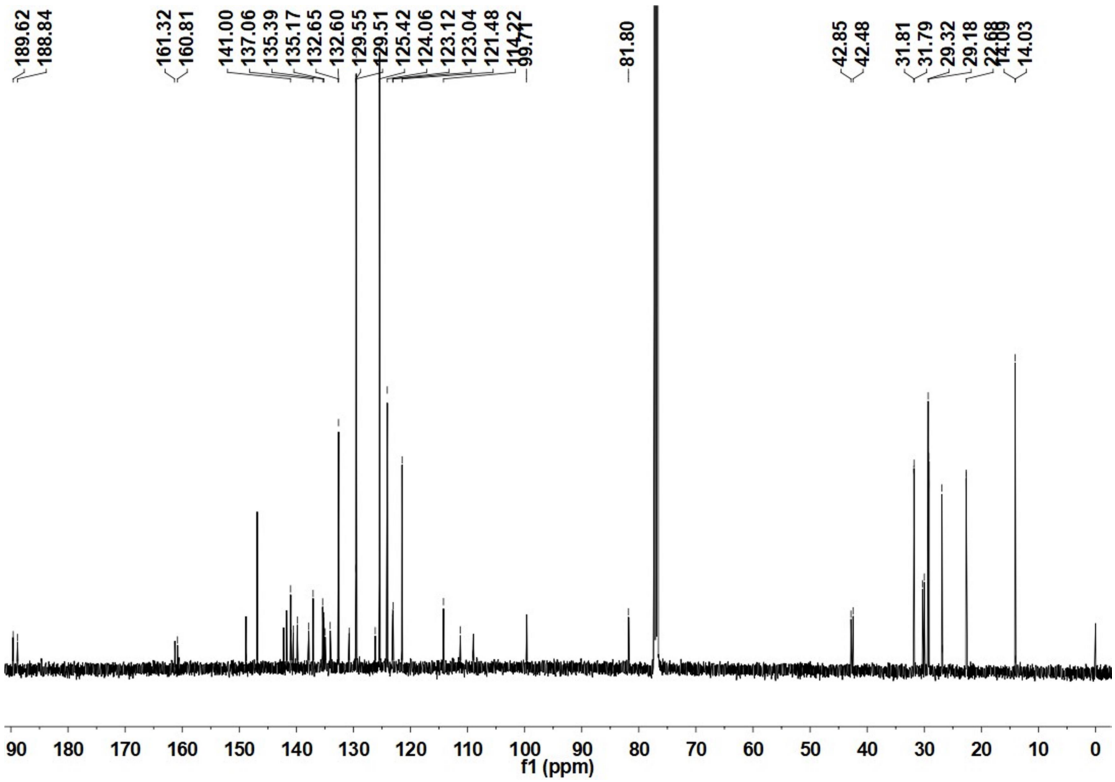

Fig. S25 ^{13}C NMR spectrum of **DPP-3**

3. TD-DFT calculated electronic transitions

Density functional theory (DFT) and time-dependent density functional theory (TD-DFT) calculations were accomplished by Gaussian 09 software at the Becke's three-parameter gradient-corrected functional (B3LYP) with a polarized 6-31G(d) basis.[2]

Table S1 The theoretical calculated electronic transitions for the five compounds.

Compound	State	E^{opt} (eV)	λ (nm)	f	Composition
BT-1	S1	1.99	621	1.1705	HOMO → LUMO (70%)
	S5	3.19	388	0.5034	HOMO →LUMO+2 (63%)
BT-2	S1	1.86	665	1.2889	HOMO →LUMO (70%)
	S8	3.31	374	0.6066	HOMO →LUMO+2 (64%)
DPP-1	S1	1.84	672	1.7196	HOMO →LUMO(70%)
	S6	3.16	392	0.3431	HOMO-2 →LUMO (57%)
DPP-2	S1	1.60	773	1.7214	HOMO →LUMO (70%)
	S13	3.10	400	0.4075	HOMO →LUMO+2 (45%)
DPP-3	S1	1.69	733	1.7214	HOMO →LUMO (70%)
	S11	3.25	381	0.4881	HOMO →LUMO+3 (59%)

4. Gibbs energy of charge separation (ΔG_{SC})

As shown in **Fig. 4(b)**, ΔG_{SC} is a parameter used to describe the driving force of exciton separation at the D-A interface, and when the value is greater than 0.3 eV, the efficient free charge carrier can be expected. [3, 4] The energy gap (E_{CT}) between the HOMO level of electron donor and LUMO level of electron acceptor is related to the open-circuit voltage V_{OC} value of the OPV device. [3] The ΔG_{SC} values of five target compound are calculated according to the following formulas[3, 5]:

$$\Delta G_{SC}^{e} = E_g(D) + IP(D) - EA(A) \quad (1)$$

$$\Delta G_{SC}^{h} = EA(A) - E_g(A) - IP(D) \quad (2)$$

The term where, E_g represents the optical band gap of target compound and $PC_{61}BM$ (1.8 eV) [5]; IP(D) is the ionization potential of target compound (approximately equal to $-E_{HOMO}$); EA(A) is the electron affinity of $PC_{61}BM$ (approximately equal to $-E_{LUMO}$). [5] The data are summarized in **Table 2.** As shown in **Table 2**, theΔG_{SC} values for the target compounds are much higher than 0.3 eV, providing sufficient driving forces for the exciton dissociation of D-A interface. Although the ΔG_{SC}^{e} value of the DPP-based molecules is lower than that of the BT-based molecules, the DPP-based molecules exhibits narrow optical bandgap and stronger optical absorption range, which increases the probability that the excitons generated in the active layer of the OPV will be dissociated into a charge carrier. On the other hand, the ΔG_{SC}^{h} value of the DPP-based molecules is higher than that of the BT-based molecules. Thus, hole transfer will be more efficient in the DPP-based molecules.

Table S2 The data of ΔGSC predicted for PV devices based on SMs: PC61BM and the energy of charge-transfer state (E_{CT})

Compounds	ΔG_{SC}^{e} (eV)	ΔG_{SC}^{h} (eV)	E_{CT} (eV)
BT-1	0.9	0.7	1.11
BT-2	0.8	0.7	1.13
DPP-1	0.5	0.8	0.97
DPP-2	0.5	0.8	0.96
DPP-3	0.5	0.8	0.95

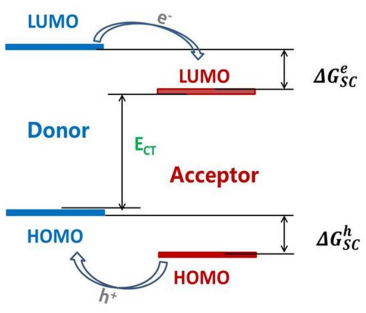

Fig. S26 Schematic diagram of the ΔG_{SC} (Gibbs energy of charge separation)[5].

5. *J-V* curves of the PV devices based on SMs:$PC_{61}BM$ active layers under an illumination of AM 1.5G, 100 mw cm^{-2} and in the dark

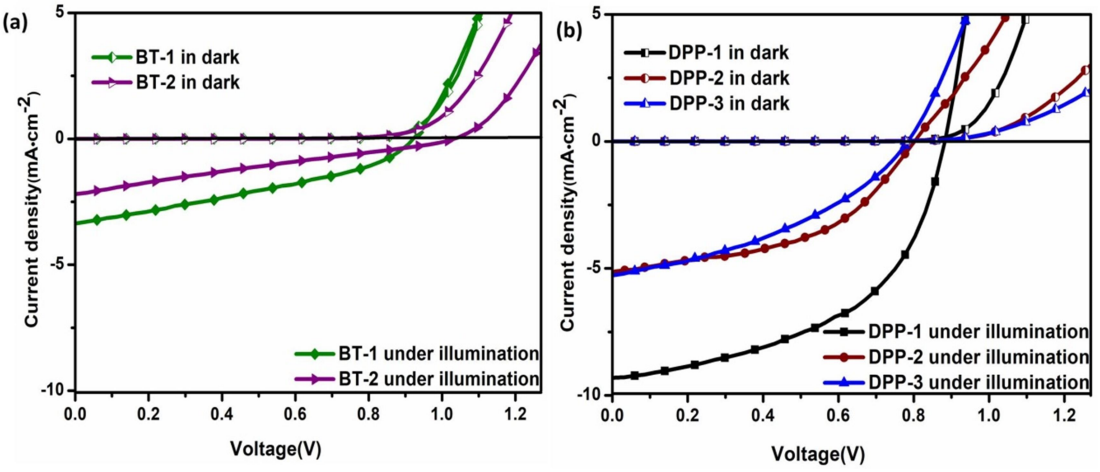

Fig. S27 *J-V* curves of the PV devices based on SMs:$PC_{61}BM$ active layers under an illumination of AM 1.5G, 100 mw cm^{-2} and in the dark

6. Preliminary PV parameters of the devices based on P3HT:BT-1 and P3HT:BT-2 active layer

Table S3 Preliminary PV parameters of the devices based on P3HT:**BT-1** and P3HT:**BT-2** active layer.

Compound (SMs)	Concentration (mg mL-1)	P3HT:SMs (w/w)	V_{OC} (V)	J_{SC} (mA·cm^{-2})	FF	PCE (%)
BT-1	9	1:3	0.78	2.05	0.24	0.39
BT-2	9	1:3	0.56	3.08	0.30	0.52

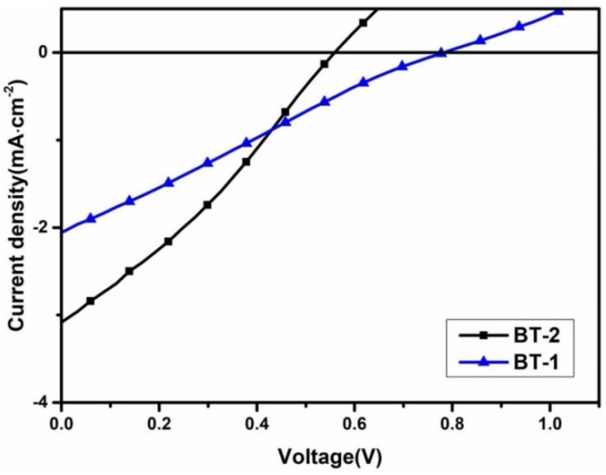

Fig. S28 *J-V* curves of the devices based on P3HT:**BT-1** and P3HT:**BT-2** active layer.

7. DSC curves of the target compounds

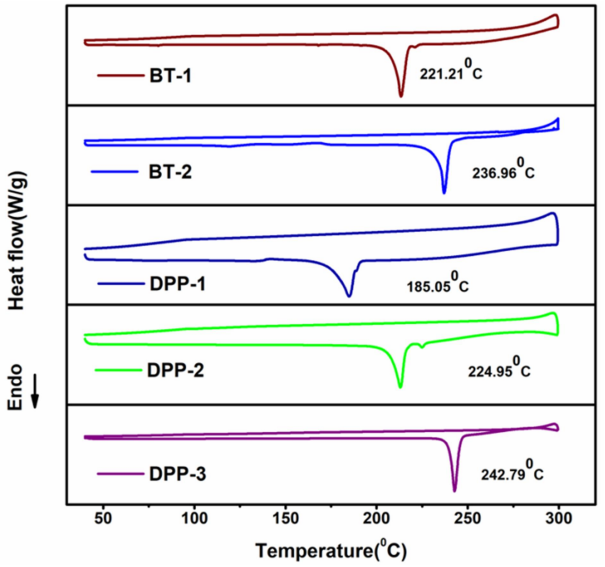

Fig. S29 DSC curves of five target compounds.

8. Atomic force microscopy (AFM) image

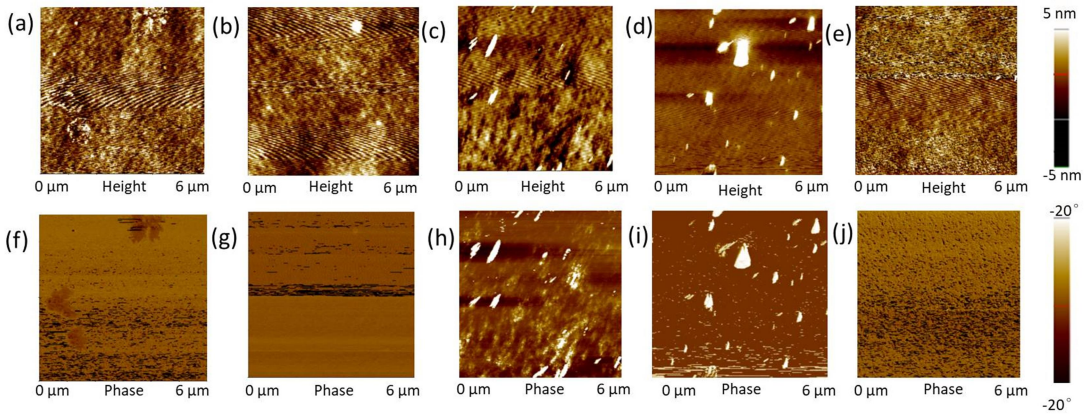

Fig. S30 (a)–(e) AFM height images; (f)–(j) AFM phase images for **BT-1**:$PC_{61}BM$, **BT-2**:$PC_{61}BM$, **DPP-1**:$PC_{61}BM$, **DPP-2**:$PC_{61}BM$ and **DPP-3**:$PC_{61}BM$ blend films**.**

In order to investigate the surface and bulk morphologies of the blend films, atomic force microscopy (AFM) measurement was employed. As shown in **Fig. S30**, the film of **BT-1**:$PC_{61}BM$ showed phase separations with a root-mean-square surface roughness (R_q) of 1.09 nm, whereas that of **BT-2** had a uniform and smooth surface with a R_q of 1.20 nm and the network interpenetrating structure was not obvious, which probably caused inefficient charge separation and transport, resulting in their low PCEs. However, the **DPP-1** based OPV showed a fine networked interpenetration structure with a R_q of 1.48 nm and achieved the best PCE among these devices. In addition, compared to the blend film of DPP-1, the blend film of DPP-2 and DPP-3 showed phase separations with a R_q of 1.69 nm and 1.88 nm respectively, the increased phase separation may hinder the charge transmission at the D-A interface, thus affecting the device efficiency.

9. References

1. X. He, L. Yin and Y. Li, *New J. Chem.*, 2019, 43, 6577-6586.
2. C. Ji, L. Yin, K. Li, L. Wang, X. Jiang, Y. Sun and Y. Li, *RSC Adv.*, 2015, 5, 31606-31614
3. P. Heinrichová, J. Pospíšil, S. Stříteský, M. Vala, M. Weiter, P. Toman, D. Rais, J. Pfleger, M. Vondráček, D. Šimek, L. Fekete, P. Horáková, L. Dokládalová, L. Kubáč and I Kratochvílová, *J. Phys. Chem. C*, 2019, 123, 11447-11463.
4. L. J. A. Koster, S. E. Shaheen and J. C. Hummelen, *Adv. Energy Mater.* ,2012, 2, 1246-1253.
5. D. C. Coffey, B. W. Larson, A. W. Hains, J. B. Whitaker, N. Kopidakis, O. V. Boltalina, S. H. Strauss and G. Rumbles, *J. Phys. Chem. C*, 2012, 116, 8916-8923